# Atomistic-Level Modeling for Thickness Dependence of Electron Mobility in InSb QW-FETs

Ximeng Guan, Jing Lu, Yan Wang, and Zhiping Yu
Institute of Microelectronics
Tsinghua University
Beijing 100084, China
gxm@mails.tsinghua.edu.cn

***Abstract*—The thickness dependence of electron mobility in the InSb quantum well (QW) FETs are calculated based on an atomistic approach for bandstructure calculation. The electron effective mass ($m^*$) is computed using fast yet accurate $sp^3d^5s^*$ tight-binding (TB) method for InSb quantum-well (QW) (or ultra-thin-body, UTB) with thickness of 3-16 nm. The $m^*$ dependence on the UTB thickness is then used in determining the electron mobility in the channel region of InSb QW-FETs. It is found that in QW-FETs, optical phonon scattering is a dominant factor, which is in turn strongly coupled to the carrier effective mass determined by channel thickness. The thickness dependence of electron mobility differs from that of the MOSFETs, where surface roughness is one of the major scattering mechanisms,**

***Keywords - mobility; Indium Antimonide (InSb); ultra-thin-body (UTB); bandstructure; effective mass.***

## I. INTRODUCTION

InSb quantum-well (QW) transistors formed by AlInSb/InSb heterostructures are under spotlight recently due to its remarkable potential in low power/voltage and high-speed circuits [1]. It has been observed that to achieve the same performance as the state-of-the-art silicon MOSFETs, InSb QW-FETs consume about 10% in power owing to extremely high electron mobility (as high as 30,000 $cm^2$/V-s) and saturation velocity ($5\times10^7$ cm/s) in the channel region [2]. Although electron mobility for bulk InSb has already been studied, the modeling of effective electron mobility for InSb QW transistors calls for additional effort in two aspects. First, the quantum confinement in the thickness direction needs to be correctly and accurately calculated. Second, the difference in the scattering mechanisms of a InSb QW transistor from those of bulk materials should be studied. The difference in scattering mechanisms between InSb QW and Si MOSFETs have been studied in [3]. However, the strong quantum confinement in a nanoscaled InSb ultra-thin-body (UTB) and its impact on electron mobility needs further discussion.

In this paper, the mobility of two-dimensional electron gas (2DEG) in InSb QW is calculated based on the bandstructure computation using the $sp^3d^5s^*$ TB method [4]. The effective mass obtained is then used to determine the polar optical phonon scattering rate, which dominates the electron mobility. It is found that as the layer thickness decreases, so does the electron mobility in InSb channel region.

## II. DEVICE STRUCTURE

The depletion mode InSb QW-FET studied in this paper is illustrated in Fig. 1. A $\delta$ doped AlInSb barrier layer saves the carriers from Coulomb scattering caused by ionized impurities and provides carriers in channel at a zero gate voltage. The transistor thus works in a depletion mode with carriers confined in the InSb QW, as shown in Fig. 2. The device structure is also known as a modulation doped field-effective-transistor (MODFET). It has been demonstrated that when the mole fraction of Al increases to 30%, the electron wavefunction is perfectly confined in the well [2]. Therefore, surface roughness scattering does not play a major role in determining the carrier mobility in the channel [3], in contrast to surface mode devices like Si MOSFETs.

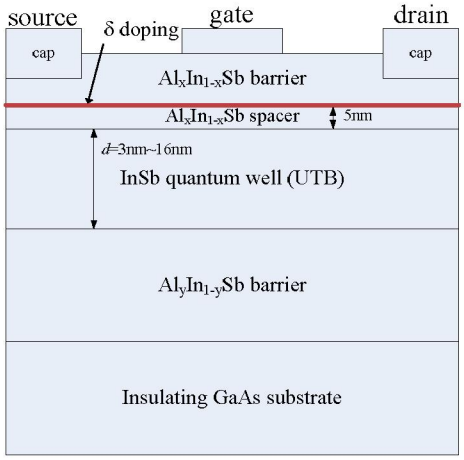


Figure 1. The AlInSb/InSb Quantum Well Transistor studied in this work. The mole fraction of Al in the barrier layer is set to 30% (i.e., $x = y = 0.3$).

## III. APPROACHES

Different approaches have been developed for carrier mobility simulation. One of the most commonly adopted schemes is based on the Monte Carlo method, which randomly select from different scattering mechanisms at the end of each free flight. The mobility calculated then converges to a constant value after enough time of simulation. Although the

This work is supported by a grant from National Science Foundation in China (Computational Nanoelectronics, # 90307016). The grant from Foundation for Ph.D. studies of Chinese Ministry of Education is also greatly appreciated.

 

method has been approved for accurate mobility calculation, it does not relate the average electron mobility and scattering probability for each mechanism in an analytical way, and thus does not give a direct insight into the impacts of different scattering mechanisms and potential changes caused by bandstructure distortion.

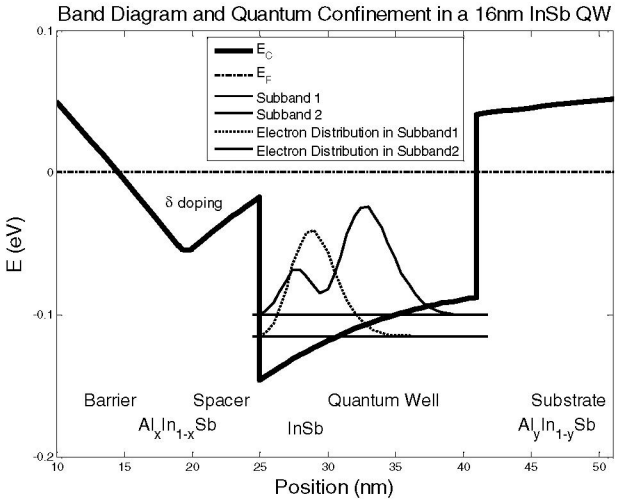


Figure 2. Conduction band diagram of a 16nm QW-FET at thermal equilibrium. Penetration of wavefunction into the spacer is negligible.

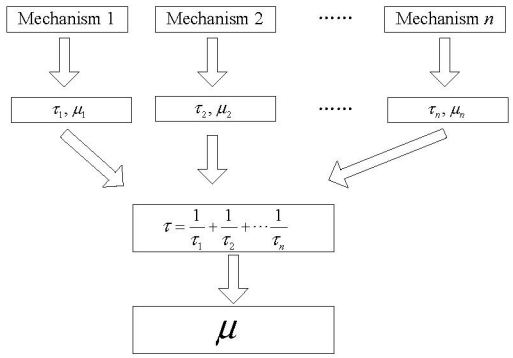


Figure 3. The scheme for mobility calculation in this work. Electron scattering mechanisms are considered separately and corresponding values of lifte time are caculated to generate a total life time for the mobility calculation.

In this work we choose a simple scheme, which calculates electron life time for different scattering mechanisms separately. The average life time and total electron mobility are then calculated by combining the life time of all mechanisms in an analytical way. The process is shown in Fig. 3. Compared with the Monte Carlo scheme, this approach may not give mobility values with the same accuracy. However, this analytic approach provides a clear vision of the combination and interaction between the scattering mechanisms. So it enables us to determine the dominant mechanism, and find out to which degree the electron mobility is changed due to quantum confinement effect. Thus this approach gives a quick and reasonable estimation of the trend of electron mobility.

According to [3] and [5], scattering mechanisms shown in Fig. 3 include those from remote impurities in the barrier, background impurities in the QW, and phonons along the 2-dimensional lattice. Alloy-disorder scattering and surface roughness scattering are neglected, as both of them do not dominate the scattering of electrons in a depletion mode quantum well transistor. As we do not apply a high vertical electric field, the electron-electron scattering is also neglected as the gate-voltage induced sheet charge density is relatively lower. For each scattering mechanism, the electron life time is evaluated. Fig. 4 shows the electron mobility ( $\mu_i$ ) due to different scatterings vs. sheet charge density. It is observed that at room temperature, the dominant scattering is from polar optical phonons. Electron lifetime and mobility corresponding to this type of scattering can be approximated by [3]

$$\tau_{\text{polar}} = \frac{2\hbar^2\varepsilon_p(e^{\frac{E_{\text{op}}}{k_B T}}-1)}{\pi\sqrt{2E_{\text{op}}}(m^*)^{1/2}q^2} \propto (m^*)^{\frac{-1}{2}}, \Rightarrow \mu_{\text{polar}} = q\frac{\tau_{\text{polar}}}{m^*} \propto (m^*)^{\frac{-3}{2}}, \quad (1)$$

where $$\frac{1}{\varepsilon_p} = \frac{1}{\varepsilon_\infty} - \frac{1}{\varepsilon_r} \quad (2)$$

with $\varepsilon_\infty$ the high frequency dielectric constant and $\varepsilon_r$ the static dielectric constant. $E_{op}$ is the optical phonon energy and $q$ is the charge of an electron. It is seen from (1) that in contrast to surface roughness scattering, $\mu_{\text{polar}}$ is a strong function of (inversely proportional to) electron effective mass (EM) to the power of 3/2, but a weak function of carrier concentration, which is quite different from that of the Si channel in a MOSFET. Traditional bandstruture calculation methods like the effective mass (EM) approach treat the electron effective mass as a constant in a low dimensional structure. However, this approximation leads to great errors in Si UTBs when the thickness is below 4nm, as has been pointed out by Rahman [6]. As the electron effective mass is lower in bulk InSb than that in bulk Si, the relative change of effective mass is expected to be even greater when the thickness is reduced to nanoscale. Thus the sensitivity to the change of EM caused by quantum confinement in the thickness direction becomes the leading factor in device scaling and cannot be neglected.

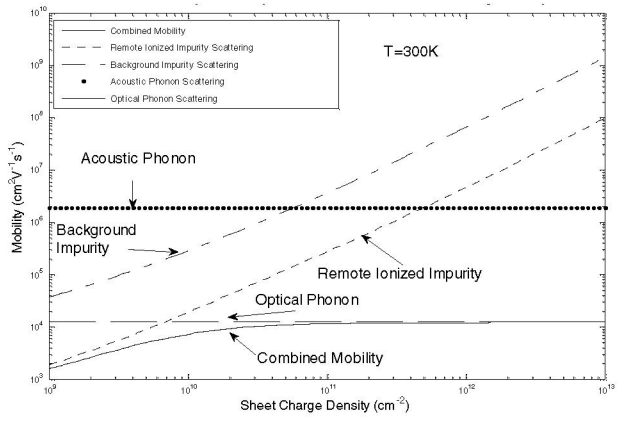


Figure 4. Electron mobility of an InSb UTB (16nm) due to different scatterings vs. sheet charge density ($n_s$). It can be seen clearly that at room temperature, optical phonon scattering dominates the total scattering rate for $n_s > 10^{10}$cm$^{-2}$. The data are based on formulas in [3].

In this work, we employ an atomistic approach in bandstructure calculation, based on the $sp^3d^5s^*$ tight-binding model. The approach has been successfully applied in Si/Ge nanowires [7], and Fig. 5 shows its application in an InSb UTB with 6 atom layers. Table 1 shows the Hamiltonian matrix of this UTB, resulting from our approach.

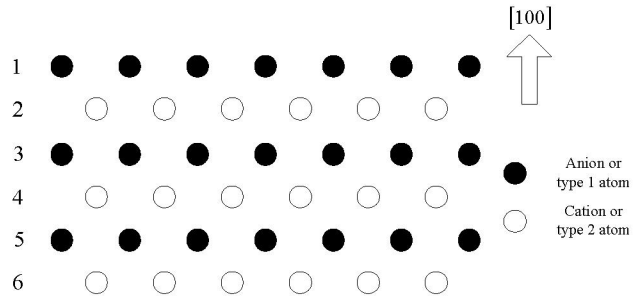


Figure 5. The scheme for mobility calculation in this work. Electron scattering mechanisms are considered separately and their lifte time is caculated to generate a total life time for the mobility calculation.

TABLE I. HAMILTONIAN MATRIX OF THE UTB SHOWN IN FIG. 3

| | | | | | |
|---|---|---|---|---|---|
| $BC_a$ | $D_{down}(k)$ | | | | |
| $D^H_{down}(k)$ | $E$ | $D^H_{up}(k)$ | | | |
| | $D_{up}(k)$ | $E$ | $D_{down}(k)$ | | |
| | | $D^H_{down}(k)$ | $E$ | $D^H_{up}(k)$ | |
| | | | $D_{up}(k)$ | $E$ | $D_{down}(k)$ |
| | | | | $D^H_{down}(k)$ | $BC_c$ |

Each cell in Table 1 is a $20\times20$ submatrix. The 6 columns/rows in Table 1 correspond to the 6 layers in Fig. 3. The interactions between the nearest atom layers, i.e., the chemical bonds between anions and cations, correspond to the off-diagonal submatrices in the table (i.e., $D_{down}(k)$ and $D_{up}(k)$ ). $E$ and $BC_{a,c} = E + B_{a,c}$ are corresponding onsite energy matrix of each inner layer and boundary condition matrices of the two interface layers. It is seen that the whole matrix is a function of $k$. For each $k$ in the first Brillouin zone (BZ), the eigen values of the Hamiltonian matrix are calculated to generate bandstructure of the UTB.

It can be seen from Table 1 that the TB approach we have employed has a resolution of finding bandstructure change due to a single atom layer variation in UTB thickness, thus much more accurate than the EM approach which treats the channel as a continuous and infinitely dividable body. The Hamiltonian matrix is diagonalized at each k point in the BZ to get bandstructures of the InSb UTB. Effective mass is then extracted for different QW thickness.

Because the dependence of electron mobility on sheet charge density ($n_s$) is weak, as shown Fig. 4, Taurus [8] is employed in estimating sheet charge densities for different gate voltages.

## IV. RESULTS AND DISCUSSIONS

Fig. 6 shows the 2D bandstructure and density of states of InSb QWs calculated by the $sp^3d^5s^*$ tight-binding approach with different thicknesses [9]. Conduction band distortion at $\Gamma$ can be evaluated by electron effective masses. It is observed that for a 3nm InSb UTB, the electron effective mass is $0.055m_0$, wheares that for bulk is $0.0135m_0$. Similar calculations were performed for 16nm and 5nm QWs, and $0.017m_0$ and $0.032m_0$ are found, respectively, for EM values at $\Gamma$. Thus when the QW thickness decreases from 16nm to 3nm, electron EM grows by more than 3 times in the transport plane.

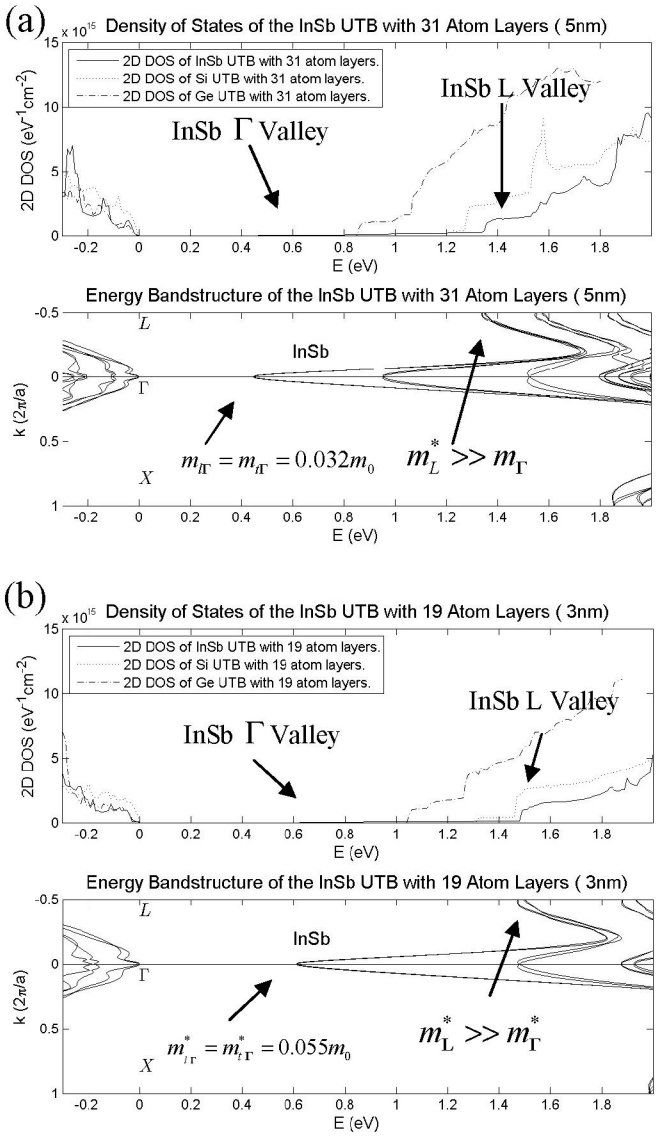


Figure 6. Density of states and bandstructure of (100) InSb UTBs, with (a) 31 atom layers (5nm), and (b) 19 atom layers (3nm). By comparing with those of Ge and Si, it is seen that (100) InSb UTBs have direct band gap. The electron EM at $\Gamma$ is about 2~4 times of bulk InSb's EM ( $m^*_{bulk\Gamma} = 0.0135m_0$ ).

One may argue that because different dielectric constants have been reported for InSb in (1) ($\varepsilon_\infty$ and $\varepsilon_r$) [3] [10], it may lead to uncertainty in determining the value of electron mobility. However, the $(m^*)^{-3/2}$ dependence of mobility dominated by polar optical phonon scattering is undistrurbed. We thus plot the normalized values to illustrate relative degradation of electron mobility with the layer thickness in Fig. 7. The weak concentration dependence of electron mobility validates our employment of Taurus as a first-order estimator for sheet charge density ($n_s$).

Fig. 7 shows that according to our calculation, the electron mobility decreases as the thickness of the UTB increases. This is due to the increase of effective mass when quantum confinement induces distortion in the conduction band valley. However, the quantum box in Taurus which is based on the effective mass approximation indicates that the mobility increases when the channel thickness is shrunk from 15nm to 3nm.

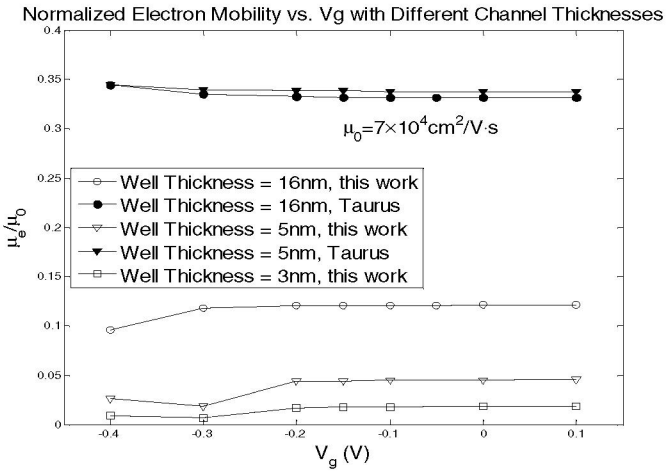


Figure 7. Normalized electron mobility vs. Vg with different thicknesses. Taurus' prediction neglects change in the effective mass caused by the quantum confinement and thus fails to predict the mobility degradation when the QW thickness decreases (3-16nm in this work). In our work, we neglect the effect of vertical field on electron mobility, as the transistor is a depletion mode device and surface scattering is not dominating the transport of electrons. The results from Taurus validate the approximation we take.

It is seen from Fig. 7 that the mobility does not exceeds $10^4$cm$^2$/Vs. However, experiments by Datta [1] have shown a measured electron of mobility of 32000 cm$^2$/Vs. We find that the relatively smaller mobility calculated by us is due to the approximations used in deriving the analytic expression for electron lifetime in (1), which leads to an asymptotic behavior towards a low mobility limit of electron mobility in Fig. 4. For more accurate modeling, a self-consistent simulation of gate stack and the Monte Carlo scheme need to be incorporated.

## V. CONCLUSIONS

We calculated electron mobilities for InSb QW's with different thicknesses. It is found that while the device channel scales and the thickness decreases, increase of effective mass caused by quantum confinement may cause significant degradation in the electron mobility. Thus to model the nanoscale InSb devices, quantum effects need to considered in a more accurate way, which makes atomistic tight-binding method a candidate approach to generating bandstructure parameters for transport simulation of low dimensional nanoscale devices.

## REFERENCES


[1] S. Datta, T. Ashley, J. Brask, L. Buckle, M. Doczy, M. Emeny, D. Hayes, K. Hilton, R. Jefferies, T. Martin, T. J. Phillips, D. Wallis, P. Wilding, and R. Chau, "85nm gate length enhancement and depletion mode InSb quantum well transistors for ultra high speed and very low power digital logic applications," IEDM Technical Digest, pp. 763-766, 2005.

[2] T. Ashley, A. R. Barnes, L. Buckle, S. Datta, A. B. Dean, M. T. Emeny, M. Fearn, D. G. Hayes, K. P. Hilton, R. Jefferies, T. Martin, K. J. Nash, T. J. Phillips, W. H. A. Tang, P. J. Wilding, and R. Chau, "Novel InSb-based quantum well transistors for ultra-high speed, low power logic applications," 7th Int'l Conf. on Solid-State and Integrated Circuits Technology (ICSICT) Proceedings, vol. 3, p. 2253-2256, 2004.

[3] Y. Shao, and S. A. Solin, "Carrier mobilities in delta-doped heterostructures," *ArXiv Condensed Matter e-prints*, 0602140, 2006.

[4] J. Jancu, R. Scholz, F. Beltram, and F. Bassani, "Empirical spds* tight-binding calculation for cubic semiconductors: general method and material parameters," Phys. Rev. B, pp. 6493-6507, 1998.

[5] J. H. Davies, The Physics of Low-Dimensional Semiconductors: an Introduction, Cambridge University Press, 1998.

[6] A. Rahman, G. Klimeck, T. B. Boykin, and M. Lundstrom, "Bandstructure effects in ballistic nanoscale MOSFETs," IEDM Technical Digest, pp. 139-142, 2004.

[7] X. Guan, and Z. Yu, "Supercell approach in tight-binding calculation of Si and Ge nanowire bandstructures," Chin. Phys. Lett., vol. 22, pp. 2651-2654, 2005.

[8] Taurus Device Userguide, Synopsys, 2003.

[9] X. Guan, and Z. Yu, "Atomistic approach to thickness-dependent bandstructure calculation of InSb UTB," IEEE Trans.Nanotechnol., unpublished.

[10] Ö. Özbaş, and M. Akarsu, "Monte Carlo simulation of electron transport in InSb," Turk. J. Phys., vol. 26, pp. 283-287, 2002.